TU Delft

Delft University of Technology

Document Version
Final published version

Licence
Dutch Copyright Act (Article 25fa)

Citation (APA)
Prosperi, A., Longo, M., Korswagen, P. A., Korff, M., & Rots, J. G. (2026). Development of Fragility Curves for Historical Masonry Buildings on Strip Foundations Exposed to Subsidence Using NLFE Models. In S. Saloustros, & K. Beyer (Eds.), *Structural Analysis of Historical Constructions: SAHC 2025, Volume 1* (pp. 972-985). (RILEM Bookseries; Vol. 64). Springer. https://doi.org/10.1007/978-3-032-13469-1_77

Important note
To cite this publication, please use the final published version (if applicable).
Please check the document version above.

Copyright
In case the licence states “Dutch Copyright Act (Article 25fa)”, this publication was made available Green Open Access via the TU Delft Institutional Repository pursuant to Dutch Copyright Act (Article 25fa, the Taverne amendment). This provision does not affect copyright ownership.
Unless copyright is transferred by contract or statute, it remains with the copyright holder.

Sharing and reuse
Other than for strictly personal use, it is not permitted to download, forward or distribute the text or part of it, without the consent of the author(s) and/or copyright holder(s), unless the work is under an open content license such as Creative Commons.

Takedown policy
Please contact us and provide details if you believe this document breaches copyrights.
We will remove access to the work immediately and investigate your claim.

This work is downloaded from Delft University of Technology.

Development of Fragility Curves for Historical Masonry Buildings on Strip Foundations Exposed to Subsidence Using NLFE Models

Alfonso Prosperi[1(✉)], Michele Longo[1], Paul A. Korswagen[1], Mandy Korff[1,2], and Jan G. Rots[1]

[1] Faculty of Civil Engineering and Geosciences, Delft University of Technology, Stevinweg 1, 2628 Delft, The Netherlands
a.prosperi@tudelft.nl

[2] Deltares, P.O BOX, 177, 2600 MH Delft, The Netherlands

Abstract. This paper presents a framework for developing fragility curves for masonry buildings on strip foundations exposed to subsidence using non-linear finite element (NLFE) analyses. A 2D plane-stress model of a masonry façade is used to evaluate the probability of cracking damage resulting from settlements. The model simulates the behaviour of typical Dutch two-storey historical buildings, using an established modelling approach to represent the non-linear behaviour of the façade, the transversal walls and the strip foundation, supported by a base interface for soil-foundation interaction. Settlements are imposed at the bottom of the interface, characterizing their intensity with the angular distortion. The damage severity is objectively quantified using the scalar parameter Ψ, computed considering the number, length, and width of the cracks.

Cumulative probability functions are derived from 864 numerical analyses that account for realistic variations in building and soil features, including 3 masonry materials, 2 strip foundation systems, 2 interface soil materials and the 72 possible settlement patterns. The effect of each selected variation is evaluated individually. The proposed curves reveal a probability of over 25% for cracks up to 5 mm in width when the angular distortion equal to 0.2% (or 1/500), the threshold deemed acceptable by international codes, is applied to the models. Doubling the applied angular distortion results in an approximate doubling of the probability of damage. While the proposed curves are specific to the selected geometry, the framework can be adapted to accommodate different façade geometries, enabling the development of more comprehensive fragility functions.

Keywords: settlements · numerical modelling · masonry structures · damage · fragility curves

1 Introduction

Historical unreinforced masonry buildings on shallow foundations are particularly vulnerable to ground settlements, which can lead to both non-structural damage, such as damage to finishes or windows, and structural damage, such as cracks in load-bearing

© The Author(s), under exclusive license to Springer Nature Switzerland AG 2026
S. Saloustros and K. Beyer (Eds.): SAHC 2025, RILEM Bookseries 64, pp. 972–985, 2026.
https://doi.org/10.1007/978-3-032-13469-1_77

walls. This is a significant issue in regions like the Netherlands, where ongoing land subsidence increases the risk of damage to structures. In this context, assessing the probability of damage to existing historical structures is required for risk and cost-benefit analyses.

Masonry buildings in the Netherlands typically feature thin façades with large openings [1, 2]. Structures built before 1960 often feature double-wythe walls, or cavity walls, with inner and outer leaves made of clay bricks [3, 4]. Moreover, a survey from the Council for the Environment and Infrastructure (*De Raad voor de leefomgeving en infrastructuur* in Dutch, Rli [5]) revealed that about 70% of the buildings in the Netherlands rest on shallow foundations, directly exposed to settlements.

Considering the inherent uncertainties and variability in real-world building conditions, such as construction materials, degradation level, foundation systems, and soil properties, it is essential to account for these factors to probabilistically assess the response of structures subjected to settlements. This challenge represents the central focus of this research.

2 Methodology and Set-Up of the Numerical Models

To estimate the probability of different damage levels in historical masonry façades subjected to settlements, modelling techniques established in earlier studies [6–9] have been employed. The 2D plane-stress model represents a façade on strip foundations subjected to soil distortions that lead to a loss of support, while allowing the structure to deform in response (Fig. 1). The application is presented with reference to the façade of a farmhouse built in 1883, already used in prior research [9–12]. The façade is a double wythe wall with a thickness of 210 mm. Previous research also provides insights into typical settlement patterns of masonry walls, for example, through measurements of bed joint levels [13–16]. The intensity of the applied settlement is quantified by the angular distortion, i.e. the slope of the line joining two consecutive points in relation to a line joining the two points at the sides of each settlement profile [17]. The angular distortion β is herein considered to be the maximum along the settlement pattern.

The methodology adopted in this study consists of two steps:

- In Step 1, the 2D NLFE models are built with the finite element software DIANA FEA 10.8 [18]. The computational models are detailed in Sect. 2.1.
- In Step 2, cumulative density functions are computed using the angular distortion β as the demand parameter: cumulative density functions are obtained by counting the number of analyses that reach a certain damage severity for each value of applied angular distortion.

2.1 Set-Up of the NLFE Models

The modelling strategy employs a 2D plane stress-structural model that integrates both the façade and foundation. It accounts for the stiffness and weight effects of the transversal walls and foundations using the approach described in [6, 8]. The non-linear shear, crushing, and cracking behaviour of the masonry material are modelled using a homogenized continuum. A non-linear interface is used at the bottom of the foundation to

simulate the interaction with the shallow soil stratum. The soil-foundation interface properties are defined based on the mechanical parameters of the soil. Settlements are applied at the bottom of the interface.

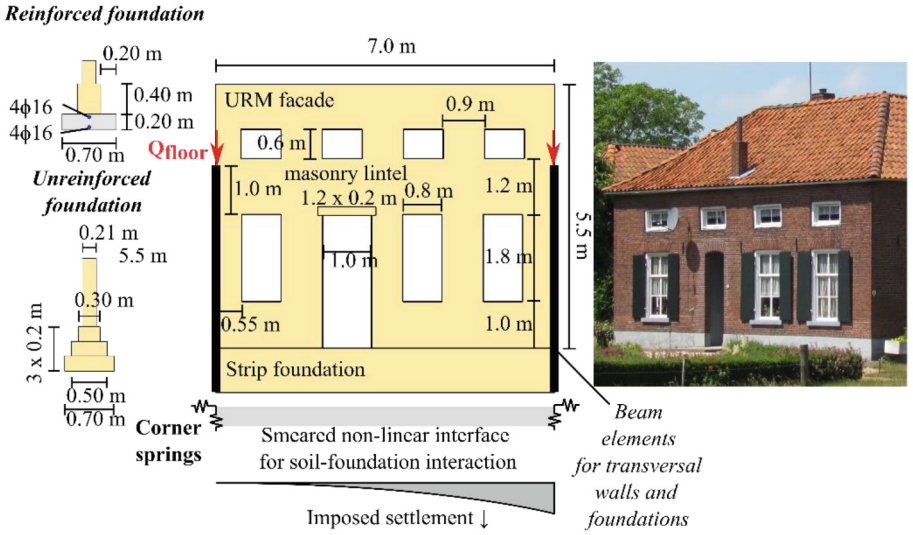


Fig. 1. The geometry of the adopted 2D modelling approach. The photo on the right depicts a typical farmhouse façade as an example, retrieved from [9, 19].

To obtain probabilistic relationships, realistic variations of settlement patterns (72), soil parameters (2), strip foundation systems (2), and masonry materials (3) are used to generate 864 analyses. With these analyses, probabilistic relationships for the façade can be derived, and the individual impact of each variation can be explored. These variations contribute to creating more realistic and comprehensive results by capturing the potential range of responses that structures may exhibit under different scenarios. According, the considered variations are detailed in the following.

Two strip foundation systems are selected for the analyses:

- An unreinforced masonry strip foundation (Fig. 1), featuring a stair-stepped cross-section that progressively increases with depth.
- A reinforced concrete (RC) strip below a masonry beam in Fig. 1.

The base interface uses the Coulomb-friction model, whereas the values of the vertical and horizontal stiffness are determined for each soil material with the formulation reported by [20, 21]. The interface stiffness values depend on soil shear modulus G, Poisson's ratio ν, and the foundation's footprint area. Moreover, the Coulomb-friction interface requires the definition of the friction angle. According, two soils are considered in the analyses:

- Sand, characterized by a shear modulus G of 35 MPa, the Poisson's ratio equal to 0.30 and a friction angle of 30°;

- Clay, characterized by a shear modulus G of 10 MPa, the Poisson's ratio equal to 0.45 and a friction angle of 15°;

Vertical and horizontal supports are thus applied at the bottom of the interface elements. Two corner springs located beneath the transverse walls are used to model the soil-structure interaction for the transverse walls [6, 8].

The non-linear cracking behaviour of the masonry material is modelled using an orthotropic, smeared crack/slip/crush constitutive law, specifically the Engineering Masonry Model (EMM) [22, 23]. The EMM incorporates both horizontal and vertical tensile softening, as well as shear and crushing softening. The parameters of the adopted constitutive law for clay brick masonry are reported in Table 1 [22, 24, 25]. In particular, three material property sets are used: "Standard" material, a "Weak" material, in which the properties of the standard material are reduced, and a "Strong" material, in which the properties are increased. The EMM is adopted for the masonry façade, lintels and foundation.

For the lateral elements positioned at the sides of the façades to simulate the effect of the stiffness and weight of the transverse walls, the Total Strain Rotating Crack Model (TSRCM) is used for the masonry material, as the EMM cannot be used for the beam elements. According, the Poisson's ratio is set to 0.25 to ensure that the shear modulus G matches that of the EMM material. The TSRCM retains the same mass density as the EMM, while the tensile strength f_t values correspond to the f_{ty} values specified for the EMM in Table 1. For the reinforced concrete foundation, the non-linearity of concrete is also modelled with the TSRCM. The Von Mises Plasticity model is used for the steel material of the rebar in the RC foundations. The material properties are reported in Table 2. The steel used for the rebars in the case of reinforced concrete foundations has Young's modulus equal to 210 GPa and yield stress equal to 235 MPa.

Plane-stress elements with an average mesh size of 200 × 200 mm are used for the façade, foundation, and lintels. The model employs 8-node quadratic quadrilateral elements with a 3 × 3 Gaussian integration scheme, along with 6-node quadratic triangular elements featuring 4 Gaussian points. Class-III Mindlin beam elements are positioned along the sides of the façade and foundation to capture the effects of the transverse walls and transverse foundations. The line interface elements utilize 3 + 3 node elements with a Newton-Cotes (5-point) integration scheme, while the corner interfaces employ 1 + 1 node elements.

Table 1. The material parameters of the EMM corresponding to clay brick masonry adopted in the FE models

Material Properties	Symbol	Unit of measure	Weak	Standard	Strong
Young's modulus vertical direction	E_y	MPa	2500	5000	7500
Young's modulus horizontal direction	E_x	MPa	1250	2500	3750
Shear Modulus	G_{xy}	MPa	1000	2000	3000
Bed joint tensile strength	f_{ty}	MPa	0.050	0.100	0.150

(*continued*)

Table 1. (*continued*)

Material Properties	Symbol	Unit of measure	Weak	Standard	Strong
Minimum strength head-joint	$f_{tx,\ min}$	MPa	0.075	0.150	0.225
Fracture energy in tension	$G_{ft,I}$	N/m	2.6	10.0	22.4
Angle between stepped crack and bed-joint	α	rad	0.5	0.5	0.5
Angle between stepped crack and bed-joint	α	rad	0.5	0.5	0.5
Compressive strength	f_c	MPa	4.25	8.50	12.75
Fracture energy in compression	G_c	N/mm	16.76	18.39	19.90
Friction angle	φ	rad	0.64	0.64	0.64
Cohesion	c	MPa	0.075	0.150	0.225
Fracture energy in shear	G_s	N/mm	0.025	0.100	0.224
Mass Density	ρ	Kg/m3	1900	1900	1900

Table 2. Adopted material properties for the reinforced concrete in the numerical models.

Material Properties	Symbol	Unit of measure	Concrete
Young's modulus	E	MPa	32000
Poisson's ratio	ν	–	0.2
Fracture energy in tension	$G_{ft,I}$	N/mm	0.137
Compressive strength	f_c	MPa	33
Tensile strength	f_t	MPa	2.565
Mass density	ρ	Kg/m3	2350

2.2 Applied Loads and Settlement

In the model, gravity loads and settlements are applied. Gravity loads include both the self-weight of the structure and the overburden, which is modelled with two forces applied to the top of the transverse walls (Fig. 1). These forces, each equal to 8.86 kN, represent the load of the floor and roof on the transverse walls, whereas the façade is non-loadbearing.

The imposed settlement patterns are modelled as vertical displacements imposed at the bottom nodes of the base interface. The displacement patterns conformed to a Gaussian curve, based on equation Eq. (1) reproduce measured building deformations, such as the ones in [13, 26].

$$S(x) = (-1)^t \left\{ e^{\left[\frac{-(x-D_x)^2}{2x_i^2} \right]} \right\} \tag{1}$$

The parameters in Eq. (1) correspond to:

- S(x) is the vertical displacement along the direction "x", parallel to the façade.
- "D_x" is the horizontal distance between the symmetry axis of the Gaussian curve and the edge of the building;
- "x_i" is the distance from the symmetry axis of the curve to the point of inflexion;
- "ι" is a binary parameter, either equal to 0 or 1, term that enables controlling the convexity of the Gaussian curve.

72 settlement shapes are derived based on arbitrary combinations of D_x, x_i, ι, as shown in Fig. 2. For each shape, the maximum angular distortion along the settlement pattern is set to 1/300 (or 3.33‰).

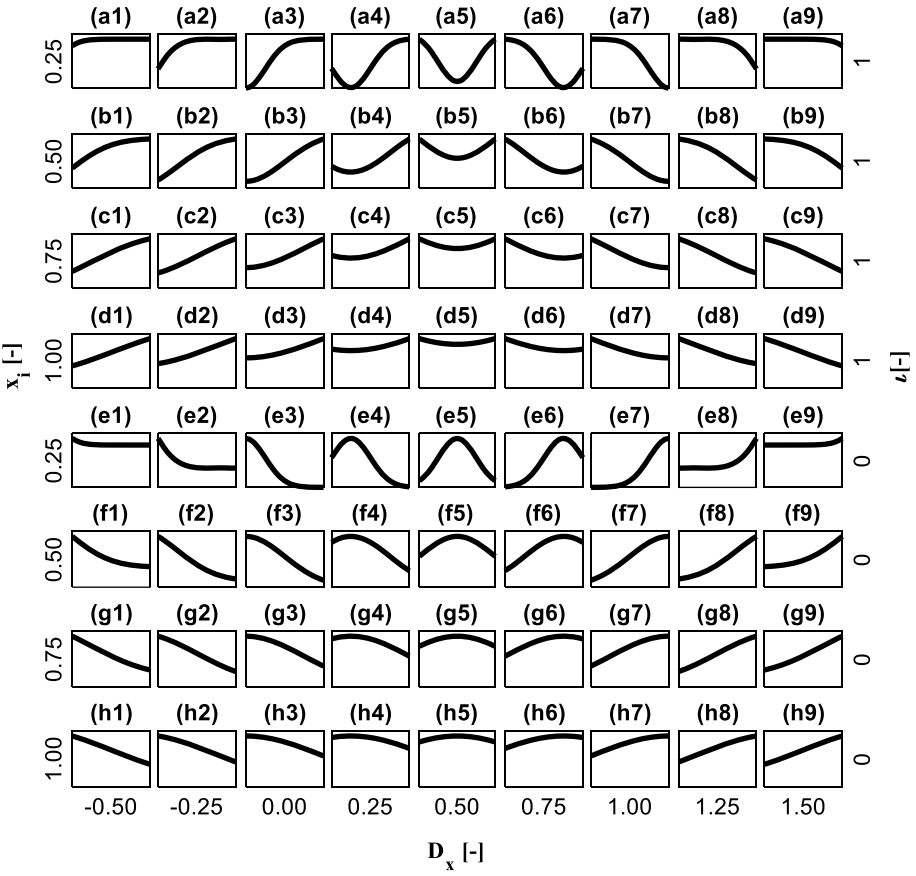


Fig. 2. The derived settlement shapes adopted in the numerical analyses are based on arbitrary intervals of the parameters D_x, x_i and ι.

A two-step procedure is used for the application of the loads in the FE analyses:

- First, gravity is applied to the structure to compute the stress states due to the self-weight and overburden. The two actions are applied separately with 10 steps each. After completing these 20 steps, the resulting displacement field of the façade is reset to isolate and track the displacement field caused solely by the settlement loading.
- Then, the settlement patterns are applied as prescribed nodal displacements at the bottom of the interface elements. The number of steps used for the application of the settlements differs per shape (i.e., for each shape in Fig. 2). Settlement shapes with more pronounced curvature require a lower maximum settlement, and thus fewer steps, to achieve the target angular distortion. Each settlement pattern is applied by progressively increasing the displacement with load increments of 0.2 mm/step. In this way, the angular distortion is progressively increased from 0 (in the first step after the application of the gravity load) up to a maximum of 1/300.

2.3 Damage Assessment

In this study, cracking damage is automatically and objectively assessed using a parameter (Ψ) proposed by [27, 28] that includes the crack width, length, and number. This parameter is calculated from the tabulated outputs of the FE analyses, which provide the crack width information for each integration point of the façade. Ψ is limited to the assessment of the light damage, i.e., up to cracks of about 5 mm wide, whereas damage that could affect the structural safety would require a different metric, possibly quantifying the reduction of the capacity of the structure. A summary of the relation between Ψ and the approximate crack width for the various damage levels is presented in Table 3.

Table 3. Damage scale with the classification of visible damage and the corresponding discretization of the damage parameter Ψ, from [27–30].

Damage level	Degree of damage	Approximate crack width	Parameter of damage
DL0	No Damage	Imperceptible cracks	$\Psi < 1$
DL1	Negligible	up to 0.1 mm	$1 \leq \Psi < 1.5$
DL2	Very slight	up to 1 mm	$1.5 \leq \Psi < 2.5$
DL3	Slight (end of light damage)	up to 5 mm	$2.5 \leq \Psi < 3.5$
DL4	Moderate (No longer light damage)	5 to 15 mm	$3.5 \leq \Psi < 4.5$
DL5	Severe	15 to 25 mm	$4.5 \leq \Psi < 6.0$
DL6	Very Severe	Above 25 mm	$\Psi \geq 6.0$

3 Results

The results of the 864 analyses, considering the different selected combinations of 3 masonry materials, 2 soil materials, 2 foundation systems and 72 settlement shapes, are used to retrieve the cumulative density functions shown in Fig. 3. The cumulative density

curves represent the ratio between the number of analyses that reach a specific level of damage (indicated by the Ψ values, ranging from 0.5 to 3.0 in increments of 0.5) and the total number of analyses, for a given angular distortion β.

The curves resemble S-shaped distributions, beginning with a flat initial portion, followed by an increase in the probability of damage, and eventually reaching an upper plateau, where further increases in applied distortion do not significantly affect the probability of damage.

For all damage severities, in the slope region, i.e., the part of the curves where the probability of damage progressively increases, doubling the applied angular distortion corresponds to nearly doubling the probability of damage. For instance, for Ψ = 1.0, corresponding to the onset of visible cracking damage, the probability of damage transitions from 40% to 70% as the applied angular distortion increases from 1/1000 to 1/500. Similarly, for the same values of applied β and Ψ = 3.0, the probability increases from approximately 10% to 25%.

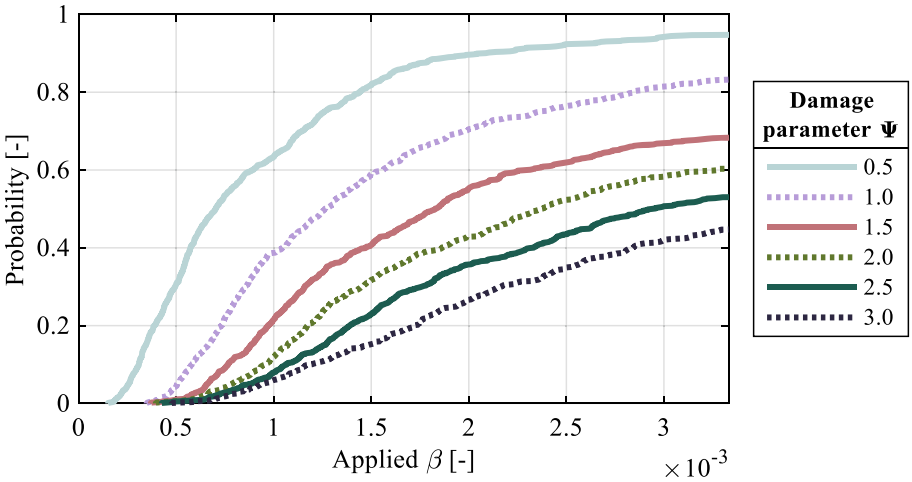


Fig. 3. The cumulative density curves in terms of applied angular distortion against the probability of damage, including the results of 864 FE analyses.

Overall, none of the models exhibits any visible damage (Ψ = 1.0) damage for values of the applied β lower than 1/3000. Slightly less than 20% of the models do not achieve visible damage even for an applied β of 1/300, as seen in the part of the graph above the Ψ = 1.0 curve. This results from favourable combinations of the selected parameters. However, slightly more than 40% of the models show cracks up to 5 mm (Ψ = 3.0), indicating the transition to structural damage rather than just light damage. For an applied angular distortion of 1/500 (2.00‰), this percentage is approximately 25%. While in the Eurocode [31] it is reported that "*A maximum relative rotation of 1/500 is acceptable for many structures*", about one-quarter of the analyses herein presented exhibit damage at the threshold of structural damage. However, at this level of damage, cracks in structural walls may not compromise the safety of the structure, supporting

the validity of the threshold proposed by the guidelines. Additionally, differences exist between the applied β and the one computed from the façade deformation, as previously reported in [7]. Therefore, the validity of the threshold may still hold, but further analyses are necessary. Nevertheless, the analyses herein presented provide a warning against the use of deterministic thresholds without considering the inherent uncertainty and variability of real-world structures.

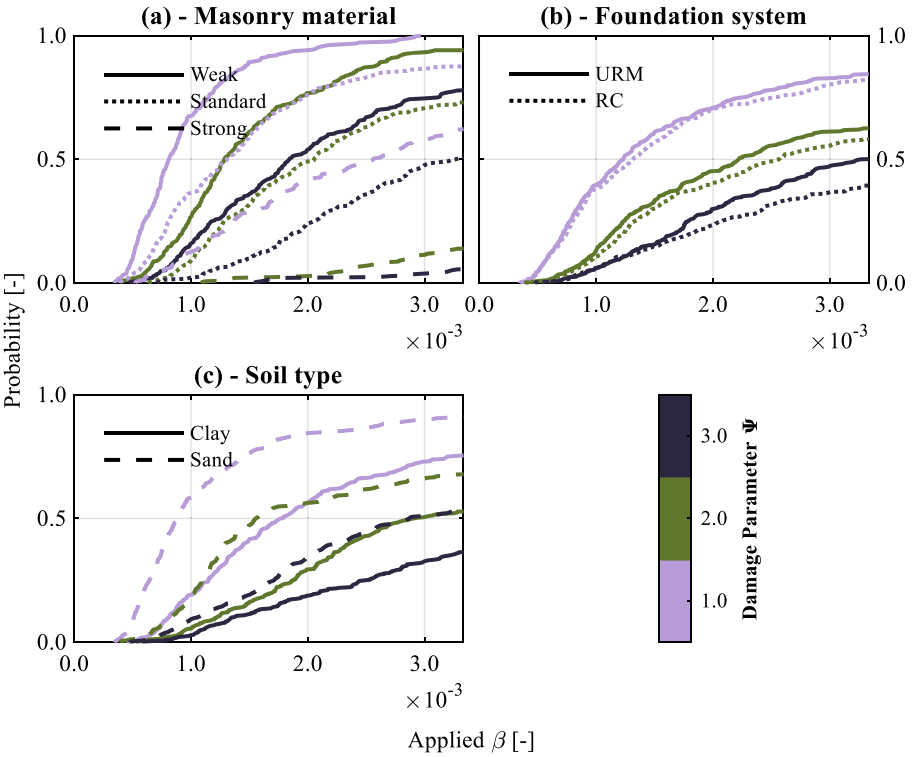


Fig. 4. Cumulative density functions in terms of applied β segregated by: (a) masonry material, (b) foundation system and (c) soil type.

Given the number of FE analyses, it is possible to examine the effects of the chosen masonry material, foundation system, and soil type on the cumulative density curves separately. The cumulative density functions are thus segregated based on each selected variable in Fig. 4, focusing on the curves for $\Psi = 1.0$, 2.0 and 3.0 for clarity. The curves confirm how a weak masonry material makes the models more vulnerable to soil distortion (Fig. 4a). Interestingly, only 5% of the models with strong masonry material exhibit cracks up to 5 mm, whereas this percentage is 50% for standard masonry and almost 80% for weak masonry.

In Fig. 4b the effect of the two selected foundation systems is shown. For low values of applied β, the differences between reinforced concrete (RC) and unreinforced foundations are not particularly significant. These differences become more pronounced at higher values of applied angular distortion, although they remain limited to no more than 10%. This is due to the limited distance between the rebar and the small concrete cross-section, which may not significantly increase stiffness compared to URM foundations. Additionally, the reinforcement bars mainly affect the model's response in sagging settlement profiles, where tensile stresses concentrate at the bottom of the façade. In hogging conditions, however, where tensile stresses are concentrated at the top of the façade, this beneficial effect is reduced.

In Fig. 4c, the effect of the two selected soil materials is shown. The probability of damage for "Sand" is higher than that for "Clay". Although this observation may seem counterintuitive, it accurately reflects the interaction between the stiffness of the building and that of the soil: a building is relatively less stiff on sand than on clay. As a result, the models are better able to withstand imposed distortions on clay soil compared to sand. Overall, for each value of applied angular distortion, the probability of damage for structures on sand is 1.5 times higher than for those on clay.

It is also possible to identify which settlement patterns among the 72 selected have the most detrimental effects on the façade. The area under the cumulative density curves serves as a metric to assess which settlement shapes are associated with the highest probability of damage. The cumulative density functions for each of the 72 settlement patterns for β ranging between 0 and 1/300 are calculated and their areas are summed. The results are summarized in Fig. 5.

The selected façade geometry is nearly symmetrical, so no significant difference is observed in the effects of asymmetric settlements in either direction. It can be observed that both asymmetric and symmetric hogging settlement patterns have the most detrimental effect (Fig. 5 a3, a7 and e8). Sagging settlement patterns and shapes with subtle curvature are associated with the least adverse effects. The results confirm that the selected settlement patterns represent a comprehensive range of scenarios the structure might experience, including both highly detrimental and less harmful ones.

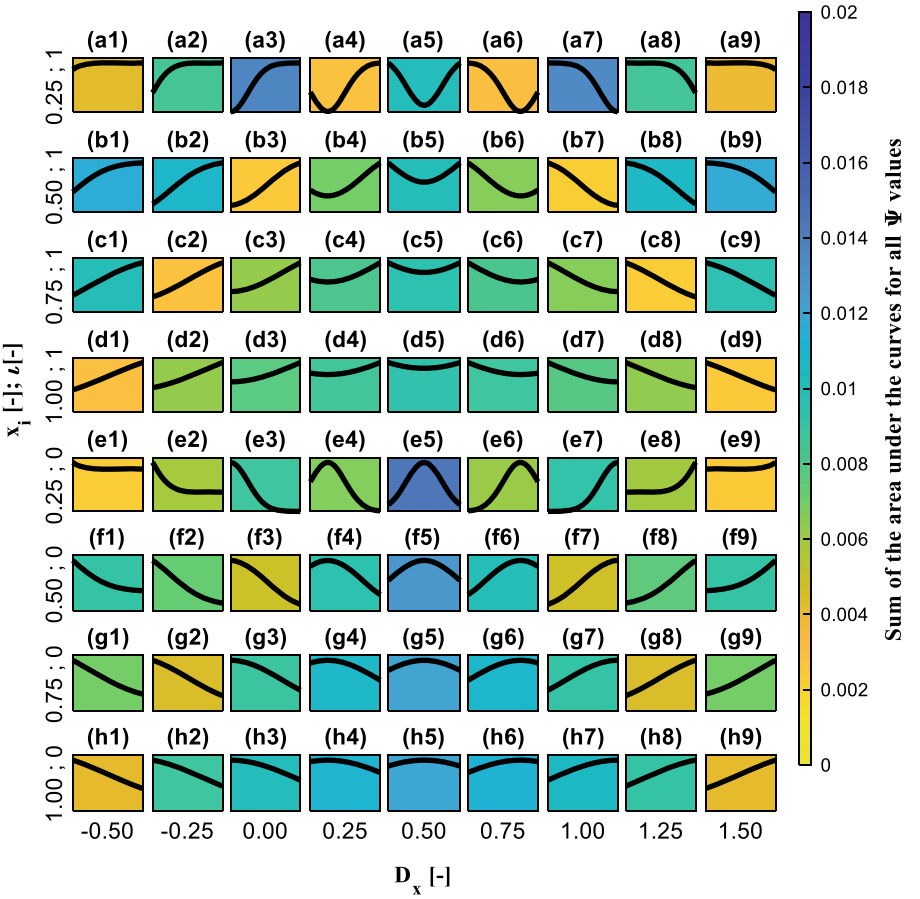


Fig. 5. The settlement shapes are distinguished by their detrimental effect in terms of damage. The sum of the areas under all the cumulative density functions from Ψ equal to 0.5 up to 3.0 obtained for each settlement shape is used to distinguish the most detrimental ones. Blue colour means a larger probability of damage.

4 Discussion and Conclusions

In this study, 2D plane-stress models are used to assess the cracking damage to historical masonry structures experiencing settlements. 2D models that account for the effects of transverse walls and foundations have been shown to reproduce the behaviour of more complex 3D models with satisfactory accuracy when settlement patterns do not exhibit 3D variations [6, 8]. If settlements exhibit 3D variations, it is expected that some façades may experience more damage while others less. The assumption that a single façade of the building can serve as a proxy for assessing the cracking damage of the entire structure is likely to result in conservative estimates. This assumption implies that the entire building will exhibit the same level of damage as the selected façade.

While the models considered here simplify reality and the complex effects of soil-structure interaction, the approach adopted successfully identifies trends and quantifies, as well as differentiates, the effects in terms of cracking damage of various parameters.

Although this study considers a wide range of vertical displacements to represent settlement, horizontal displacements are deliberately neglected. This choice stems from the fact that horizontal soil strains are typically associated with specific sources of settlement, such as tunnels, excavations, and mining activities. Their magnitude is expected to be lower for buildings settling under their weight [32]. Therefore, buildings subjected to other subsidence processes may also experience negligible horizontal strains. This observation warrants further research.

Cracking damage is used to assess the damage severity of the façade, possibly relating that to the ease of repair (Table 3) [27–30]. Toward this aim, the parameter Ψ is used to quantify the light damage. Nevertheless, different metrics, such as building strains, could be used to assess more severe damage, as cracking may not be the most accurate indicator [17, 28, 29]. Previous research has linked the use of different metrics, like strain, to the damage scale adopted here. Therefore, further research is needed on this aspect.

Angular distortion is used to quantify the imposed distortion and serves as a demand parameter in the cumulative density functions. Although other parameters could be used, such as the differential settlemetnt or the deflection ratio, previous studies have shown that angular distortion is one of the most effective parameters for measuring settlement distortion [13, 32–34].

The results of the NLFE analyses conducted herein are used to derive cumulative density functions. These curves provide insight into how many models reach a specific level of damage, further distinguishing the effects of different features. This represents a step toward defining more accurate fragility curves for buildings exposed to settlements. The adopted methodology can therefore be applied to achieve this goal.

The analyses presented herein revealed that:

- The proposed curves reveal a probability of over 25% for cracks up to 5 mm for an applied angular distortion equal to 0.2% (or 1/500). In other words, for this angular distortion, one in four models exhibits such a level of damage severity.
- Doubling the applied angular distortion results in nearly doubling the probability of damage for a specific damage state.
- For the same applied angular distortion, the models on sand are 1.5 times more likely to sustain damage than those on clay.
- The reinforced concrete foundation proved to have slightly lower probabilities (10%) than the unreinforced one. Further improvements are expected to increase the stiffness of the foundation, for instance, by increasing the vertical distance between the rebars.
- Hogging settlement shapes have been found to have more detrimental effects than sagging ones, confirming trends established in the state of the art.

While this research represents a step toward defining the probabilistic response of historical structures subjected to settlements, further refinements are needed. For example, incorporating additional façade geometries would help include more realistic scenarios, accounting for variations in shape, length, height, height-to-length ratio, as well as opening distribution, wall thickness, and overburden. While some of the considered

scenarios may be more prevalent than others, the exact distribution and correlation of these features across all buildings in the Netherlands is unknown. This highlights the need for open and accessible data containing information on existing buildings to further refine the analyses.

Acknowledgements. The research presented here is part of the NWA project Living on Soft Soils: Subsidence and Society (grantnr.: NWA.1160.18.259).

References

1. Fusco, D., et al.: Numerical study of pier-wall connections in typical Dutch URM buildings. In: 12th International Conference on Structural Analysis of Historical Constructions: SAHC, Online Event, 29 September–1 October 2021 (2021)
2. Grant, D.N., et al.: Explicit modelling of collapse for Dutch unreinforced masonry building typology fragility functions. Bull. Earthq. Eng. **19**(15), 6497–6519 (2021)
3. Messali, F., et al.: A multiscale experimental characterisation of Dutch unreinforced masonry buildings. In: 16th European Conference on Earthquake Engineering, Thessaloniki (2018)
4. Jafari, S.: Material characterisation of existing masonry: a strategy to determine strength, stiffness and toughness properties for structural analysis. Delft University of Technology: TU Delft Applied Mechanics. https://repository.tudelft.nl. Doctoral thesis (2021)
5. The Council for the Environment and Infrastructure (Rli), Goed Gefundeerd: advies om te komen tot een nationale aanpak funderingsproblematiek (2024)
6. Prosperi, A., Longo, M., Korswagen, P.A., Korff, M., Rots, J.G.: 2D and 3D modelling strategies to reproduce the response of historical masonry buildings subjected to settlements. Int. J. Archit. Herit. **19**(5), 753–769 (2025)
7. Prosperi, A., et al.: Sensitivity modelling with objective damage assessment of unreinforced masonry façades undergoing different subsidence settlement patterns. Eng. Struct. **286**, 116113 (2023)
8. Prosperi, A., Longo, M., Korswagen, P.A., Korff, M., Rots, J.G.: Accurate and efficient 2D modelling of historical masonry buildings subjected to settlements in comparison to 3D approaches. In: Endo, Y., Hanazato, T. (eds.) Structural Analysis of Historical Constructions. SAHC 2023. RILEM Bookseries, vol. 46. Springer, Cham (2024). https://doi.org/10.1007/978-3-031-39450-8_19
9. Korswagen, P.A., et al.: Modelling of damage in historical masonry façades subjected to a combination of ground settlement and vibrations. In: International Conference on Structural Analysis of Historical Constructions. Springer, Cham (2023). https://doi.org/10.1007/978-3-031-39603-8_73
10. Rots, J.G., Korswagen, P.A. , Longo, M.: Computational modelling checks of masonry building damage due to deep subsidence. Delft University of Technology (2021)
11. Korswagen, P., et al.: Supporting analyses to determine probability of damage and fragility curves due to indirect subsidence effects. Delft University of Technology. Report. 3 October 2022 (2022)
12. Korswagen, P., et al.: Appendixes to supporting analyses to determine probability of damage and fragility curves due to indirect subsidence effects. Delft University of Technology, Report (2022)
13. Prosperi, A., Korswagen, P.A., Korff, M., Schipper, R., Rots, J.G.: Empirical fragility and ROC curves for masonry buildings subjected to settlements. J. Build. Eng. **68**, 106094 (2023)

14. Charles, J.A., Skinner, H.D.: Settlement and tilt of low-rise buildings. Proc. Inst. Civil Eng.-Geotech. Eng. **157**(2), 65–75 (2004)
15. De Vent, I.A.E.: Structural damage in masonry: developing diagnostic decision support (2011)
16. De Vent, I.A.E.: Prototype of a diagnostic decision support tool for structural damage in masonry (2011)
17. Burland, J.B., Wroth, C.: Settlement of buildings and associated damage (1975)
18. DIANA FEA bv, Finite element analysis user's manual - release 10.8. 2024: Laan van Waalhaven 462, 2497 GR, The Hague, The Netherlands (2024)
19. Monumental Farmhouse, National Monument ID: 523688. Accessed Nov 2024. https://rijksmonumenten.nl/monument/523688/boerderij-met-aangrenzende-bijschuren/breedenbroek/
20. NEHRP, NIST GCR 12-917-21 Soil–structure interaction for building structures. National Institute of Standards and Technology, US Department of Commerce: Gaithersburg (2012)
21. Gazetas, G.: Foundation vibrations. In: Foundation engineering handbook, pp. 553–593. Springer (1991)
22. Schreppers, G., et al.: DIANA validation report for masonry modelling. DIANA FEA report (2016)
23. Rots, J., et al.: Thematic Keynote Computational modelling of masonry with a view to Groningen induced seismicity. in Structural Analysis of Historical Constructions: Anamnesis, Diagnosis, Therapy, Controls: Proceedings of the 10th International Conference on Structural Analysis of Historical Constructions (SAHC, Leuven, Belgium, 13–15 September 2016. CRC Press (2016)
24. NPR9998:2020en, Assessment of structural safety of buildings in case of erection, reconstruction and disapproval - Induced earthquakes - Basis of design, actions and resistances (2021)
25. Korswagen, P.A., et al.: Damage sensitivity of Groningen masonry structures–Experimental and computational studies: Stream 1 (2017)
26. Fuertes, J.: Calibrated Numerical models for masonry buildings subjected to subsidence-related ground settlements, in Civil Engineering & Geosciences. Delft University of Technology (2024)
27. Korswagen, P.A., et al.: Crack initiation and propagation in unreinforced masonry specimens subjected to repeated in-plane loading during light damage. Bull. Earthq. Eng. **17**(8), 4651–4687 (2019)
28. Korswagen, P.A.: Quantifying the probability of light damage to masonry structures: an exploration of crack initiation and progression due to seismic vibrations on masonry buildings with existing damage (2024)
29. Burland, J.B., Broms, B.B., De Mello, V.F.: Behaviour of foundations and structures (1978)
30. Grünthal, G., European macroseismic scale 1998. European Seismological Commission (ESC) (1998)
31. CEN, Eurocode 7 Geotechnical design - Part 1: General rules. Final Draft, EN 1997–1:2004 (E), (F) and (G), in European Committee for Standardization: Brussels. 2004. p. 168
32. Boscardin, M.D., Cording, E.J.: Building response to excavation-induced settlement. J. Geotech. Eng.-Asce **115**(1), 1–21 (1989)
33. Wikby, P., et al.: A grid-based methodology for the assessment of time-dependent building damage at large scale. Tunn. Undergr. Space Technol. **149**, 105788 (2024)
34. Son, M., Cording, E.J.: Estimation of building damage due to excavation-induced ground movements. J. Geotech. Geoenviron. Eng. **131**(2), 162–177 (2005)